RESISTANCE AND SEAKEEPING CFD SIMULATIONS FOR THE KOREAN CONTAINER SHIP

Barbara d'Aure, Benoit Mallol, Charles Hirsch (NUMECA Int., Belgium)

1. SUMMARY

This paper is focused on RANS simulations of Case 2.1 and Case 2.10 of the Tokyo 2015 workshop. On Case 2.1, five different grids are considered in order to assess error levels versus mesh density, for the various measured quantities. On Case 2.10, particular attention is given to the impact of the physical and numerical parameters for the seakeeping simulation.

2. INTRODUCTION

CFD is now widely used and recognized among the community of naval architects and marine engineers in complement or in replacement of the towing tank tests. It is essentially the case for resistance simulations, for full scale or model scale, appended hull or not, where expertise has reached a sufficient mature level to automate these CFD simulations. However, a rigorous V&V (verification and validation) analysis is still required, to improve Best Practice Guidelines (BPG) and comparing them with other guidelines available in the marine CFD community.

Seakeeping simulations are more challenging since they rely on Unsteady RANS and require more CPU time, the physical behavior of the ship being completely unsteady. Hence, an error on the inputs (physical or numerical) is an important waste of time and so these simulations require a particular attention.
Our experience with seakeeping simulations shows that time and space discretizations are highly connected, illustrated by the so-called Courant number. Hence, making a V&V exercise with the mesh density on seakeeping cases should also be done in correlation to a V&V exercise on time dependence, which was not requested by this workshop. However, latest guidelines resulting from such investigation have been used and are presented in this paper.

3. RESISTANCE (CASE 2.1)

3.1 Case description

Case 2.1 is computed on the model scale (LPP = 7.2786 m) KCS hull with rudder. The rudder was containing gaps that were simplified to reduce the number of cells as shown in Figure 1 (seeing the small influence of those on the results confirmed by a preliminary investigation not described in this paper).

Fig.1 Case 2.1 Geometry

Computations are done in calm water conditions, the ship being free to heave and pitch. Six Froude numbers are studied: 0.108, 0.152, 0.195, 0.227, 0.260 and 0.282.

The experimental results are provided by KRISO/NMRI and consist in the coefficient of total resistance, heave motion and trim angle versus Froude numbers. The objective for this case is to realize a verification and validation study. The validation is done compared to these experimental data. The verification is based on a mesh dependency study and Richardson based extrapolations (for each Froude number, only the mesh density is modified, all the numerical parameters are kept identical).

3.2 Mesh and solver setups

The case setup and medium mesh generation are done using FINE/Marine's C-Wizard, a plugin allowing an automatic setup of the mesh and solver parameters based on the geometry, patch names and physical inputs.

To perform the mesh dependency study, ten different meshes are generated with HEXPRESS, FINE/Marine's mesh generator. One mesh (the medium one) is built for the four highest Froude numbers and four additional declinations of this mesh are generated to perform the mesh dependency study (very coarse, coarse, medium, fine and very fine). The same is done for the two lower Froude numbers.

The ship is refined around the geometry features and a fine mesh is also generated around the free surface location, with a vertical target cell size corresponding to LOA/1000 and an aspect ratio of 128 for the two horizontal directions. A view of this mesh on the mirror plane in shown on Figure 2. For the lowest Froude numbers (Fr = 0.108 and Fr = 0.152), an additional refinement is made with an internal surface shaped using Kelvin angles with the same vertical target cell size but a smaller aspect ratio (5) to properly capture the wake field with a smaller wave length. These extra refinements can be seen on Figure 3.

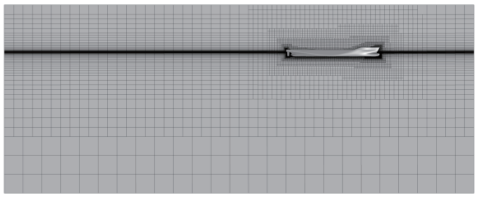

Fig.2 Mesh (mirror plane) for C 2.1 at Fr=0.282, Grid 1

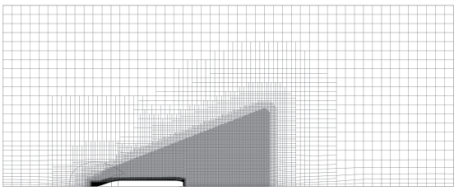

Fig.3 Mesh for lower Froude numbers (cut normal to the vertical direction), Grid 3

All refinements are done relatively to the initial mesh size. To generate meshes for the dependency study, the initial cell sizes were multiplied with successive ratios of 1.25. The viscous layer area is meshed to be compatible with a wall function (first cell size made to ensure a y+ around 50, expansion ratio of 1.2). The different numbers of cells are given in Table 1.

Table 1 Number of cells (in millions) for the mesh dependency study

Mesh density	Very coarse	Coarse	Medium	Fine	Very fine
Lower Froude	0.26M	0.80M	1.85M	3.66M	6.23M
Higher Froude	0.18M	0.49M	1.04M	1.94M	3.27M

The RANS flow solver embedded into FINE/Marine (ISIS-CFD) is used for all simulations using free-surface capturing approach (VOF method) and K-ω (SST Menter) turbulence model.

Given the symmetrical configuration, a half ship is simulated. The boundary conditions used are solid wall with wall function on the ship, prescribed pressure on the top and bottom, far field with 0 m/s velocity on the inlet, outlet and side and mirror on the symmetry plane. The velocity is imposed at the ship center of gravity. For each velocity, the ship starts from 0 m/s with an acceleration ramp (equivalent to 200 to 40 time steps). The ship heave and trim motions are solved using a quasi-static approach. For the four highest Froude numbers, a sub-cycling method on the volume fraction equation is used to reduce the computation time.

3.3 Results analysis

Tables 2 and 3 are an extract of the results submitted to the workshop. For Froude 0.282, the results for the coefficient of total resistance c_T and the coefficient of pressure resistance c_{PV} are given. The experimental value D and the relative error E%D between D and the result on each grid S are given for the coefficient of total resistance, the heave motion and trim angle. The solutions for the five different grids (Grid 1 being the finest) are given for each quantity. On Table 3, the grid ratio (r_G), the relative error between the very fine mesh (S1, on grid 1) and the fine mesh (grid 2) e_{12}%S1, the ratio between the estimated order of convergence and the theoretical order of convergence (2) p_G/p_{Gth}, the grid uncertainty U_G%S1, the EFD uncertainty U_D%D and the validation uncertainty U_V% are shown. The grid uncertainty was computed using the approach of Hoekstra & Eca (2008) for monotonic convergence. The validation uncertainty is computed as $\sqrt{U_G^2 + U_D^2}$.

Table 2 Error levels for Fr = 0.282

Parameters		EFD (D)	V&V Study				
			Grid 5	Grid 4	Grid 3	Grid 2	Grid 1 (S_1)
$C_T \times 10^3$	Value	**4.501**	4.759	4.621	4.553	4.536	4.520
	E%D		-5.729	-2.675	-1.164	-0.777	-0.411
$C_{PV} \times 10^3$	Value			1.671	1.587	1.563	1.543
	E%D						

Table 3 V&V for Fr = 0.282

Parameters		r_G	e_{12}%S_1	$p_G/p_{G,th}$	U_G%S_1	U_D%D	U_V%
$C_T \times 10^3$	Value	1.25	0.364	1.083	1.895	**1.0**	2.143
	E%D						
$C_{PV} \times 10^3$	Value	1.25	1.309	0.898	5.705		
	E%D						

On Figures 4 to 6, the relative error E%D can be seen for all Froude numbers between the experimental value D and the solution on each grid of the mesh dependency study, in function of the inverse of the cell number to the power 2/3. This study has been made for the coefficient of total resistance (Figure 4), the heave motion (Figure 5) and the trim angle (Figure 6).

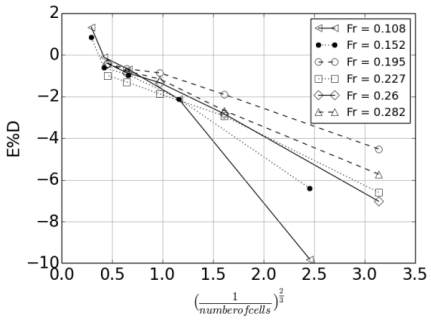

Fig.4 Mesh dependency: error on coefficient of total resistance (in %), for different Froude values

Errors on the coefficient of total resistance c_T are quite small for all Froude numbers (<1.3%*D* for the finest grid, cf. Figure 4). From an industrial point of view, to the author's knowledge, a precision below 2% on the coefficient of total resistance can be considered as satisfactory. For all Froude numbers, the relative error between the experimental results and the CFD results is below 2% for the very fine, fine and medium mesh (cf. Figure 4). Thus a medium mesh can be a good compromise between accuracy and computation speed or CPU resources. The relative error between the finest mesh and the experimental data E%D for the coefficient of total resistance c_T on the finest grid (Grid 1) is smaller than the Richardson-based validation numerical uncertainty U_V% (see Tables 2 and 3). Thus the coefficient of total resistance prediction can be considered as validated.

Concerning the coefficient of pressure resistance c_{PV}, the grid uncertainty $U_G\%S_1$ is higher than for the coefficient of total resistance c_T and the coefficient of friction resistance c_F (see Table 3, where the grid uncertainty on c_{PV} is three times higher than grid uncertainty on c_T). For this quantity, no error could be computed due to the absence of experimental data for this quantity.

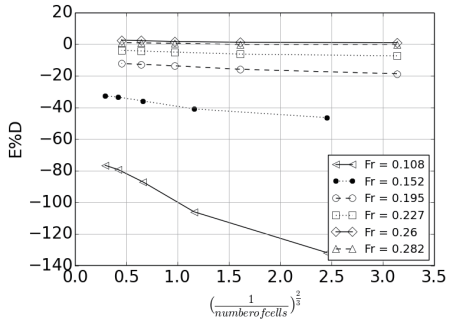

Fig.5 Mesh dependency: error on heave motion, for different Froude values

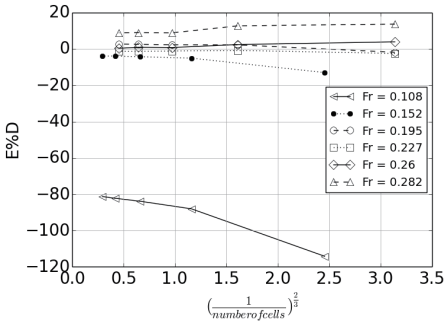

Fig.6 Mesh dependency: error on trim angle, for different Froude values

Figures 5 and 6, showing the prediction errors on heave and trim, clearly indicate that the mesh properties are not optimal for these quantities, at the lowest Froude numbers. Obviously, the mesh analysis shows that the density of mesh points around the free surface is insufficient, even on the global finer mesh. These requirements are to be introduced in the Best Practices when capturing these quantities is of importance.

The error decreases when the Froude number increases, which is probably due to the fact the motion is bigger with higher Froude numbers, thus bigger than the vertical cell size on the free surface (which is 7.5x10-3m when the heave motion for the lowest Froude is 9x10-4m). When the motion is small compared to the cell size, for example heave motion/vertical cell size around 3.4 in the most favorable case (highest Froude number), the relative error on the finest grid is small (around 1%). This could also be linked to the precision of the experimental results, the method of uncertainty analysis or a phenomenon that is not properly captured with K-ω (SST Menter) turbulence model.

Figure 7 shows the relative error for all Froude numbers between the extrapolated solution δ_{RE}, based on Richardson extrapolation, and the solution on each grid of the mesh dependency study, in function of the inverse of the cell number to the power 2/3. The least squared approach proposed by Hoekstra & Eca (2008) is used for Richardson extrapolation. This plot has been done for the coefficient of total resistance.

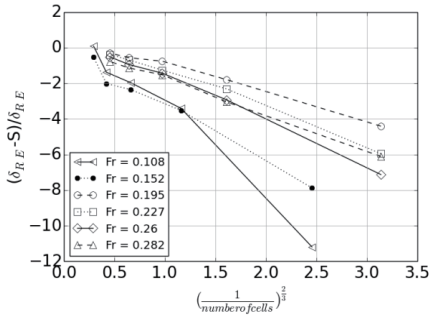

Fig.7 Mesh dependency of Richardson-based error estimation for the coefficient of total resistance

On Figures 8 to 10, the coefficient of total resistance, the heave motion and the trim angle are represented in function of Froude numbers. The black markers represent the experimental values. The empty markers connected with a plain line represent the numerical results. Uncertainty bars are plotted for both experimental (short bars, corresponding to U_D%D) and numerical (long bars, corresponding to U_G%S1) results. The trends are well captured for the three quantities. These figures allow us to confirm the observations made from Figures 4 to 6 and Tables 2 and 3.

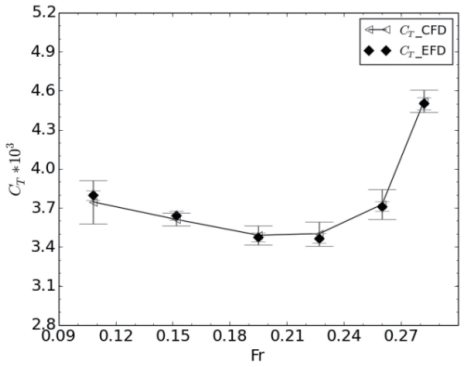

Fig.8 Coefficient of total resistance vs Froude number

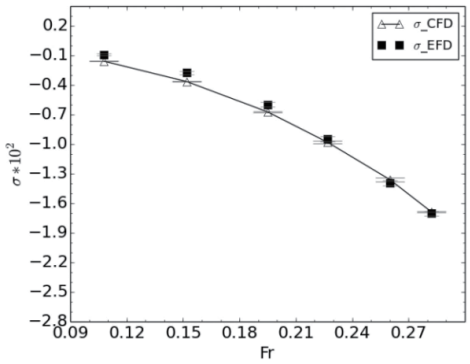

Fig.9 Heave motion (x10^2 meters) vs Froude number

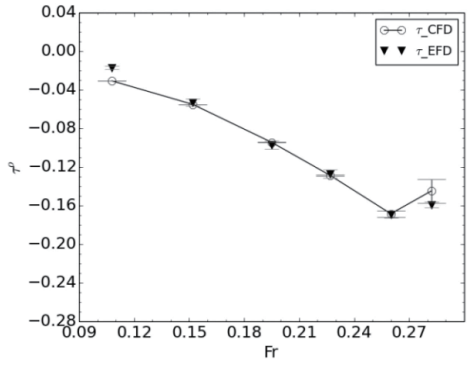

Fig.10 Trim angle (degrees) vs Froude number

4. SEAKEEPING (CASE 2.10)

4.1 Case description

Case 2.10 is computed on the model scale (LPP = 6.0702 m) KCS hull with rudder. The rudder contains gaps that were simplified to reduce the number of cells. Also the superstructure part has been removed for sake of simplification of the mesh and the simulation time, as shown on Figure 11. The authors acknowledge that for the high sea state, this could be a delicate choice since green water could be observed.

Fig.11 Case 2.10 geometry

A first computation (C0) is done in calm water condition and five computations are done in wave conditions, the ship being free to heave and pitch and the advancing speed of the ship being 2.017 m/s. Five different wave conditions are studied, as described in Table 4 with the wave length λ and wave height Hs.

Table 4 Wave conditions (wave length and wave height)

Case	C1	C2	C3	C4	C5
λ (m)	3.949	5.164	6.979	8.321	11.840
Hs (m)	0.062	0.078	0.123	0.149	0.196

Experimental results were provided by FORCE and consist in coefficient of total resistance, pitch and heave amplitude and phase harmonics and their time history.

4.2 Mesh and solver setup

The mesh for the reference calm water condition (C0) follows the strategy used for the resistance case (2.1). One mesh is done for each wave condition. Refinements are done around the free surface to capture the wave with an aspect ratio (vertical/horizontal cells size) of around 16.

For cases C3, C4 and C5, some additional refinements were done around the bulb and the aft to capture the free surface properly. The cell size in all directions corresponds to the cell size used for the free surface in the vertical direction.

Finally, a damping zone is modeled after the ship, where the cell size in the vertical direction is kept constant but the cell size in the horizontal directions is increased to damp the wave before reaching the boundary condition and avoid reflections.

A view of the mesh for case C1 is shown on Figure 12, where the refinements around the free surface and the damping area can be observed.

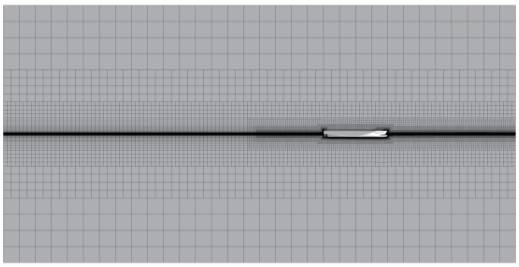

Fig.12 Mesh for case C1 (mirror plane)

The number of cells varies between 2 and 3.5M cells according to the wave specifications. C1 being the finest since it has the smallest waves height compared to ship length.

Given the symmetrical configuration, a half ship is simulated. The boundary conditions used are solid wall with wall function on the ship, prescribed pressure on the top, far field with 0 m/s velocity on the outlet, a wave generator (regular waves) on the inlet, mirror on the side patches and a solid wall with slip condition on the bottom. The velocity is imposed at the ship's center of gravity. For each velocity, the ship starts from 0 m/s with an acceleration ramp (1s) to its full speed velocity. The ships motions are solved by the Newton equations. An unsteady approach is used with a time step corresponding to 600 to 1200 time steps per wave period (1200 being used for C3 and C4). The time steps values (Δt) are presented in Table 5.

Table 5 Time steps used

Case	C1	C2	C3	C4	C5
Δt (ms)	2.65	3.03	1.76	1.92	4.59

4.3 Results analysis

Two cases will be presented here: C1 and C5, which correspond to the two extreme wave conditions proposed in the workshop. The time history reconstructed from the Fourier series is shown on Figures 13 and 14, for the heave motion, trim angle and coefficient of total resistance. Those quantities were computed at the center of gravity. They show good agreement between the experimental data (EFD) and CFD especially for C5 case. Those results show better agreement with the experiments than the raw signals, as obtained by the time dependent numerical solution. Indeed, on the raw signals, a low frequency (not represented when reconstructed from the Fourier series) is present that most probably comes from the fact the waves were generated without a ramp on the amplitude, creating a shock at the beginning of the computation and instabilities in the numerical towing tank.

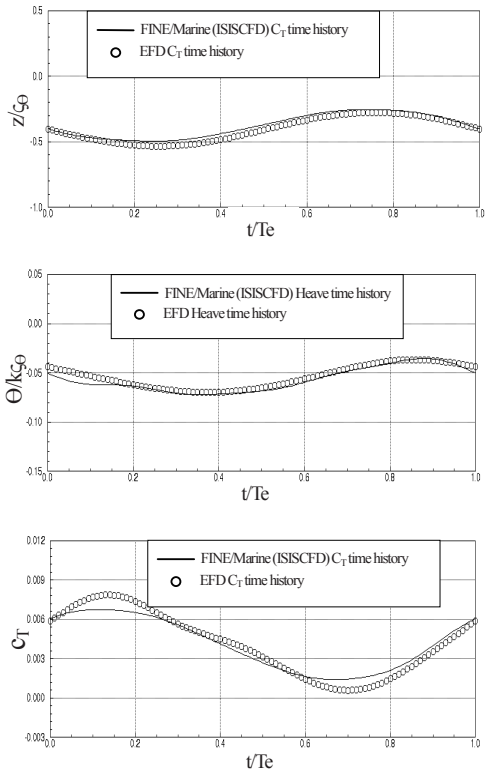

Fig.13 C1 results: time history of heave, trim angle and drag coefficients (from top to bottom), compared to experimental data

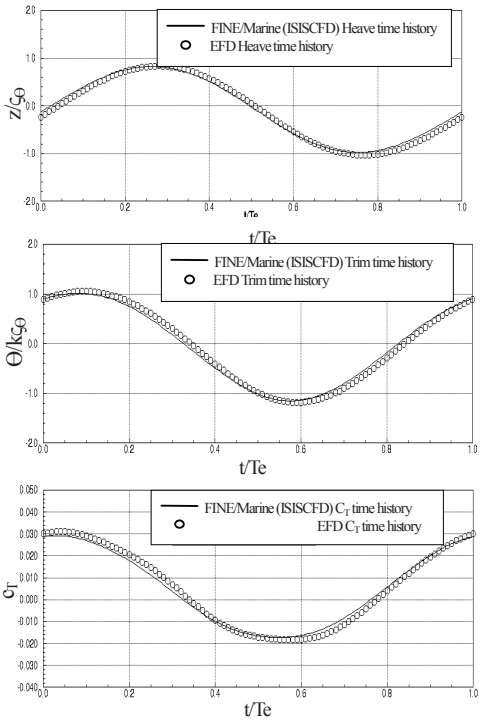

Fig.14 C5 results: time history of heave, trim angle and drag coefficients (from top to bottom) , compared to experimental data

Figures 15 and 16 shows the experimental and the CFD results amplitude of the harmonics of c_T for Case 1 (Figure 15) and Case 5 (Figure 16). On the same graph the absolute error between the experimental values and the CFD results is also shown (line). The c_T coefficient has a difference between 0.66% and 3.53% in amplitude for the 0^{th} harmonic (from C1 to C5) and between 6.58% and 17.69% for the 1^{st} harmonic (between C5 and C1). The amplitudes of the 2nd, 3rd and 4th harmonics are small compared to the amplitude of the 0th and 1rst harmonics, and are in consequence more difficult to capture. Thus even if the error on those higher harmonics is larger in terms of percentage of the experimental values for those harmonics, the absolute error is not really significant for the solution.

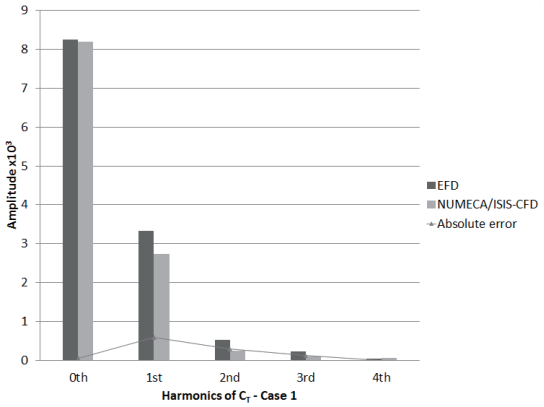

Fig.15 C1 results: harmonics of c_T

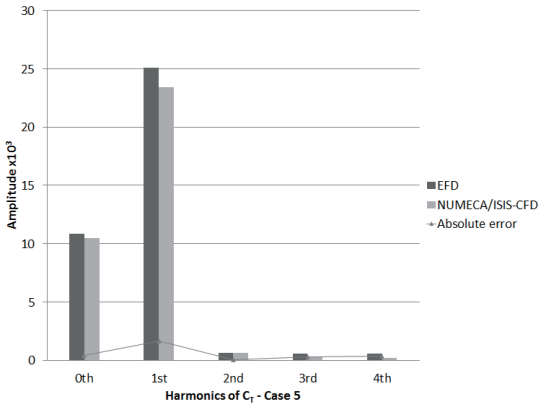

Fig.16 C5 results: harmonics of c_T

Before the submission of the results, the authors have noticed an important impact of the inertia matrix. An error of 35% can have an effect from 15% to 30% on the mean resistance depending on the case. The accuracy of the inertia matrix is of an extreme importance and should be computed with care by the experimental facilities in order to compare EFD and CFD. In this paper, the same values as in the description of the case have been used.

Besides, one question remains about the vertical position of the center of gravity since it was given at +0.093m above the free surface whereas it could be at -0.093m below the free surface according to information received by email. All the simulations in this paper have been done using the center of gravity at +0.093m (hence at 0.378m). It would be interesting as a future work to realize an uncertainty quantification study on those dynamic parameters.

5. CONCLUSION

The V&V exercise on the resistance case 2.1, shows that latest guidelines (corresponding to the medium mesh) lead to a maximum difference of 2% on the drag coefficient compared to experimental results, which was validated by the uncertainties approach. The trim angle and the heave motion are more in the range of 3-4% or more, especially at low Froude numbers where values are very small. A study of the effect of a finer mesh around the free surface area would be required to reach the same confidence as for the drag coefficient. Concerning case 2.10 (sea-keeping), first harmonics are well captured, and the error on the other harmonics has a small impact on the global solution. A time step dependency study would be required to further improve the results and the guidelines. In addition, the study has allowed to underline the importance of the physical properties of the ship such as the inertia matrix and the center of gravity, which can have a non-negligible influence on the prediction of its dynamic behavior.

ACKNOWLEDGEMENT

The authors would like to thank the developers of the FINE/Marine's flow solver ISIS-CFD from ECN (CNRS, France) for the constant support as usual.

REFERENCES

A. Leroyer, P. Queutey, E. Guilmineau, G. Deng and M. Visonneau (2009) "New algorithms to speed up RANSE computations in hydrodynamics", Proceeding of Nutts conference

B. J. Guo , G. B. Deng & S. Steen 2013, "Verification and validation of numerical calculation of ship resistance and flow field of a large tanker", *Ships and Offshore Structures* 8:1, 3-14, DOI: 10.1080/17445302.2012.669263

B.J. Guo, S. Steen, G.B. Deng 2012, "Seakeeping prediction of KVLCC2 in head waves with RANS", *Applied Ocean Research* 35 (2012) 56–67

Hoekstra M, Eca L., (2008), "Testing Uncertainty Estimation and Validation Procedures in the Flow Around a Backward Facing Step", *3rd Workshop on CFD Uncertainty Analysis*, Lisbon